INSTRUMENTATION IN THE AEROSPACE INDUSTRY - VOLUME 24

ADVANCES IN TEST MEASUREMENT - VOLUME 15

Part One

Proceedings of the 24th International Instrumentation Symposium—Albuquerque, New Mexico

1978

INSTRUMENTATION IN THE AEROSPACE INDUSTRY - Volume 24

ADVANCES IN TEST MEASUREMENT - Volume 15

Part One

Proceedings of the

24th INTERNATIONAL INSTRUMENTATION SYMPOSIUM
May 1-5, 1978
Albuquerque, New Mexico

Programmed by ISA's
Aerospace Industries Division
Test Measurement Division

Edited by
Dr. K. E. Kissell
Air Force Avionics Laboratory

INSTRUMENT SOCIETY OF AMERICA
Pittsburgh, Pennsylvania

PUBLICATION POLICY

THIRD PRINTING 1979

PART ONE

Library of Congress Catalog Card Number 68-59467

ISBN 87664-403-5

INSTRUMENT SOCIETY OF AMERICA
400 Stanwix Street
Pittsburgh, Pa. 15222

Printed in U.S.A.

INSTRUMENTATION IN THE AEROSPACE INDUSTRY - VOLUME 24

ADVANCES IN TEST MEASUREMENT - VOLUME 15

Part One

Proceedings of the 24th International Instrumentation Symposium—Albuquerque, New Mexico

1978

PAPERS FOREWARD

The 24th International Instrumentation Symposium included a four-session short course, three tutorials, one panel discussion, and nineteen papers sessions. Published here are the many papers from those sessions as well as several that were not orally presented. This volume presents the most advanced information available in the field of Aerospace Instrumentation and Test Measurements.

An undertaking as large as this results from the efforts of many people. We are grateful to all of them. The authors work is presented here, but the efforts of Session Developers and the many Chairmen should not be forgotten. A special thanks is due Allen Diercks for a truly outstanding technical program.

Jim Dorsey
General Chairman

CONTENTS

SESSION: WIND TUNNEL TESTING
Session Chairman: W. Comer

SESSION: PRESSURE AND FLOW MEASUREMENT
Session Chairman: D. W. Rockwell

SESSION: ADVANCES IN INSTRUMENTATION
Session Chairman: R. Roberts

SESSION: ELECTRO OPTICAL INSTRUMENTATION
Session Chairman: O. Freidrich

SESSION: VIBRATION MEASUREMENT
Session Chairman: R. R. Bouche

SESSION: FLIGHT TESTING

SESSION: NONDESTRUCTIVE TESTING
Session Chairman: H. S. Hayre

SESSION: ACOUSTIC EMISSION
Session Chairman: C. Bailey

SESSION: ENERGY SOURCE INSTRUMENTATION
Session Chairman: D. Davis

SESSION: RE-ENTRY VEHICLE GROUND TESTING
Session Chairman: J. Beachler

SESSION: MACHINARY INSTRUMENTATION
Session Chairman: R. Chernoff

SESSION: MASS FLOW INSTRUMENTATION FOR LOFT
Session Chairman: A. E. Arave

SESSION: RE-ENTRY VEHICLE FLIGHT TESTING
Session Chairman: R. Motensen

ISBN 87664-403-5

ADVANCES IN INTERFEROMETRIC SIGNAL ANALYSIS

S. A. Eselun and E. G. Wolff
Aerospace Corporation
El Segundo, California

ABSTRACT

Developments in phase modulation and related signal processing were applied to an automatic, real time system for monitoring two beam interference patterns.

INTRODUCTION

Analysis of optical interference patterns is a major task in such diverse fields as astronomy, metrology, vibration analysis, microscopy, shock wave research, optical fabrication and communications, and dimensional stability of materials, components and structures. Demands of improved resolution (e.g. $< \lambda/1000$), reliability and versatility lead to required signal analysis systems incorporating simultaneously, real time automated data output in digital and/or analog form, computer interfaces, bidirectional counting and fringe interpolation, fast response, and long term stability in terms of insensitivity to changes in optical alignments or transmission characteristics. In order to maintain reasonable cost it is desirable to accomplish the above with a low number of (standard) components.

The present paper describes a system suitable for the continuous measurement of a Michelson interference pattern. The automatic counting of Fabry-Perot type fringes is also possible. It is in part a homodyne technique as opposed to the generally more complex heterodyne methods.[1,2] It has been recognized[3] that phase modulation is one of the best approaches to automatic fringe counting. Indeed, directional fringe motion may be found from the integrated intensity as received by a single photodetector if the interference pattern is phase modulated. Detection of poor quality (low visibility) fringes is thereby possible with no dependence on polarization states. This is achieved by obtaining two electrical signals which are always 90° out of phase. These signals can be reliably counted with standard quadrature counters, and interpolations can be made. Extensions of this approach are best shown by reviewing the basic theory.

PHASE MODULATION OF INTERFEROMETER

The intensity from a Michelson interferometer (see Figure 1) is proportional to $(1 + \cos \delta)$ where δ is the phase difference between the two interfering beams,

$$\delta = \frac{4\pi L \nu}{c} \tag{1}$$

L is the optical path length difference
ν is the frequency of the light
c is the speed of light

If, however, one collects with a lens the entire interference field, the sinusoidal relation is preserved; and in general the intensity, I, may be expressed as

$$I = I_{dc} + I_{ac} \cos \delta \tag{2a}$$

With fringe visibility β defined as I_{ac}/I_{dc},

$$I = I_{dc} (1 + \beta \cos \delta) \tag{2b}$$

Ignoring for now the DC intensity the output voltage from a photodetector will be

$$V = V_o \cos \delta \tag{3}$$

One is interested in measuring δ and counting the number of intervening cycles at different times to get difference measurements. The counting may be achieved by generating sine/cosine signals which drive directional A quad B type counters. (Two techniques for further interpolation are discussed later). If, as mentioned, the phase is modulated by an amount, ϕ, and at frequency, ω_m, then Eqn.(3) becomes essentially (Appendix I);

$$V = V_o \cos (\delta_o + \phi \sin \omega_m t) \tag{4}$$

where δ_o is the static phase. When written in terms of Bessel functions of the first kind,

$$V = V_o J_o(\phi)\cos\delta_o + 2V_o\sum_{n=1}^{\infty}[J_{2n}(\phi)\cos\delta_o\cos 2n\omega_m t$$

$$- J_{2n-1}(\phi)\sin\delta_o\sin(2n-1)\omega_m t] \quad (5)$$

It is apparent that the quadrature signals exist in the even and odd harmonics. From Eqn. (5) the first term is used as the cosine signal; it is effectively DC. The sine signal is found by using a lock-in detector tuned to the in phase part of ω_m, n = 1. We now have the desired signals:

$$V_x = V_o J_o(\phi)\cos\delta_o \quad (6a)$$

$$V_y = -2V_o J_1(\phi)\sin\delta_o \quad (6b)$$

Figure 2 shows $J_o(\phi)$ and $2J_1(\phi)$; with no electronic manipulation equations (6) represent a circle when ϕ is chosen to satisfy the transcendental equation $J_o(\phi) = 2J_1(\phi)$. The first solution is $\phi = .896$, $J_o(\phi) = .81$. In practice, however, such a high degree of modulation is unnecessary as V_x and V_y may be adjusted to equal amplitudes electronically. For small values of ϕ, $J_o(\phi) = 1$ and $J_1(\phi) = \phi/2$, so that equations (6a) and (6b) become the original signal and its first derivative:

$$V_x = V_o\cos\delta_o \quad (7a)$$

$$V_y = -\phi V_o\sin\delta_o \quad (7b)$$

The necessary signals are achieved by amplifying V_y by an amount ϕ^{-1}.

Phase modulation may be obtained by any of three different methods. There are 1) retardation of one of the combined light beams with, e.g., an electro-optic modulator[4] or mobile grating,[5] 2) oscillation of a reference mirror by, e.g., a piezoelectric crystal[1, 3, 6] or 3) frequency modulation of the light beam.

As seen from Eqn. (1), there are two basic ways one may oscillate δ_o to obtain the phase modulation index, ϕ, namely, variation of L or ν_o.

There are also two ways one may vary L. One of these is to introduce an electro-optic modulator[4] in one of the combined light beams. The device is driven by a voltage, V_d, so that

$$\phi = \frac{\pi\nu_o K}{c} V_d \quad (8)$$

where K represents crystal parameters. This produces a change in the refractive index and therefore in L also.

Another method is to change the geometrical path by vibrating a mirror somewhere in the interferometer with a piezoelectric crystal. If the path is changed, by a peak amount, ℓ

$$\phi = \frac{4\pi\nu_o}{c}\ell \quad (9)$$

Frequency modulation is discussed in the next section and in the appendix, but if the input light beam undergoes a peak frequency deviation, ν_p, then

$$\phi = \frac{4\pi L}{c}\nu_p \quad (10)$$

It is possible that all of these could be occurring simultaneously and at different modulation frequencies in which case Eqn. (5), if expanded, would be more complex. However, if not expanded, one may consider the highest frequency as ω_m, and then choose the corresponding ϕ, whether from equation (8), (9), or (10). The quantity δ_o is time varying, and is followed by the signal processing. If all three methods were to occur at the same frequency and phase, then ϕ would be the sum of Equations (8), (9), and (10).

Each of these three methods has both advantages and disadvantages. For example, use of an electro-optic crystal in the beam path permits both mirrors (M_1, and M_2, Figure 1) to be used as the reflective ends of a test sample for contactless length measurement. However, the size of the device can sometimes make it impractical. Vibration of a mirror offers low cost and simplicity but raises the question of long term stability of the oscillating system or creep of the mirror-piezoelectric crystal interface. A mobile grating[5] is similarly subject to movement mechanism errors and also grating imperfections; however, it is insensitive to errors of alignment. The third method has not been widely attempted and is discussed separately.

FREQUENCY MODULATION BEFORE BEAM SPLITTING

Frequency modulation of the beam prior to beam splitting can also be used as a phase modulation technique (see Appendix I). In spite of similarities to Fabry-Perot work, which involves amplitude modulation[7], and heterodyne methods,[1, 2] it does not appear to have been used widely. It has been accomplished in our laboratory through the use of a Lamb dip frequency stabilized laser. The laser output mirror is mounted on the resonator housing via a piezoelectric crystal. A small amount of energy is allowed to pass through the rear reflector to a phototransistor, serving as the sensing element in the frequency stabilization loop. The processed phototransistor output is utilized as the error signal which maintains the cavity length by varying the length of the piezoelectric element. This approach has involved a 12.5 KHz signal as part of the control voltage to the output mirror crystal resulting in a frequency modulated output beam. As long as $L \neq 0$, the phase difference of an interferometer will be modulated, (Eqn. (10)). Measurements of ϕ indicate that $\nu_p \simeq$ 1MHz. This modulation has been found to work well with the signal processing system described in the next section. Figure 3 shows the change in refractive index as a vacuum system is pumped down from 760 to 10^{-3} TORR using this technique.

SIGNAL PROCESSING SYSTEM

Figure 4 shows schematically an interferometer system which we have used to measure dimensional changes in materials. Figure 5 illustrates the associated electronics. Phase modulation is induced by the mirror, M_3, driven at one of its resonances near 50 KHz. The polarizer and quarter wave retardation plates and the s/p beam splitter are used to obtain I' as well as to act as source isolation. The lock-in detector used was an Evans Associate Model 4110, especially modified to provide adequate frequency response.

The optical parameters I_{dc} and I_{ac} in Equation 2 may change during the course of an experiment. For example, oil or metallic films collecting on a vacuum window which transmits the ingoing and detected beams will cause a decrease in I_{dc}. Similarly, changes in reflectivity of the mirrors, M_1 and M_2,[3] will change I_{ac} as will slight rotations.

To compensate automatically for I_{dc}, it must be measured. This is done by introducing a second photodetector, B, which detects fringes, I', of equal visibility but shifted in phase by π with respect to those seen at photodetector A:

$$I' = I'_{dc}(1 - \beta \cos \delta) \qquad (11)$$

In converting the intensities, I and I', to voltages, V and V', variable gains, G and G', are available. Equations (2b) and (11) become

$$V = GI_{dc}(1 + \beta \cos \delta) \qquad (12a)$$

$$V' = G'I'_{dc}(1 - \beta \cos \delta) \qquad (12b)$$

These voltages are subtracted, and the gains are adjusted so that $GI_{dc} = G'I'_{dc}$, and

$$V - V' = 2GI_{ac} \cos \delta \qquad (13)$$

This signal, equal in form to Equation (3), therefore meets the requirement of being independent of I_{dc} and I'_{dc}.

Its complement is found as outlined yielding the signals, V_x and V_y. The idea is to normalize these signals so that the strength of I_{ac} becomes unimportant. This is accomplished with circuitry which for two inputs, V_x and V_y, gives as an output

$$V'_x = V_x(V_x^2 + V_y^2)^{-1/2} \qquad (14a)$$

$$V'_y = V_y(V_x^2 + V_y^2)^{-1/2} \qquad (14b)$$

With the sine/cosine form of the input signals V'_x and V'_y will be normalized to unity. In practice, about 90% of the original light source may be blocked out with no effect on these signals and, hence, measurement capability.

FRINGE INTERPOLATION

At least two techniques which use the sine/cosine signals, Eqn. (6), are available for interpolation between counts. One method is to use voltage multipliers on the original signals to find $\sin\delta\cos\delta$ and $\cos^2\delta$. These are equivalent to $\sin 2\delta$ and $\cos 2\delta$. Several stages, n, will continue doubling the phase so that the final signals are counted as before, but this time with the sensitivity increased to $\lambda/2^{n+3}$. This approach has the benefit of keeping the information digital.

Rectangular to polar conversion is considered preferable. This may be done with available integrated circuits or with a mini-computer.

CONCLUDING REMARKS

The processing of phase modulated signals as outlined here has numerous advantages. The fringe counting is reliable and the signals are easily used in feedback loops. Linear displacements, for example, can be followed from the angstrom range to the coherence length of the light source. The cost of the electronics components (about $2000) is mainly determined by the digital counter. This system can also provide digital counting of multiple beam interference patterns. This is seen by considering that when the sine/cosine signals in a two beam interference pattern are displayed on two axes of an oscilloscope, there is a circle for one complete cycle of δ_o. Applying the same procedure to Fabry-Perot transmission fringes using small oscillations, the display would appear as in Figure 6.

REFERENCES

1. Sizgoric, S., and Gundjian, A. A., (1969) "An Optical Homodyne Technique for Measurement of Amplitude and Phase of Subangstrom Ultrasonic Vibrations", Proc. IEEE p 1313-1314.

2. Tanaka, K. and Ohtsuka, Y., (1977) "Laser Heterodyne Detection of Slowly Varying Displacements", J. Optics, Vol. 8, No. 1 pp 37-40.

3. Logue, S. H., (15 Dec. 1967) "Laser Interferometry Measuring System for Precision Gyro and Gas Bearing Parts", Final Report under Contract NAS8-20568, C. C. Marshall SFC, Also General Dynamics Report GDC-DBE-68-005.

4. Yariv, A., (1971) "Introduction to Optical Electronics", Holt, Rinehart and Winston Inc. p 236.

5. Grosmann, M. and Meyrueis, P., (1977) "High Accuracy Holographic Length Comparator using Phase Heterodynage", Proc. SPIE Vol. 122 (Advances in Laser Engineering) pp 53-62.

6. Zakharov, V. P. et alia, 1976 "Limiting Sensitivity and Accuracy Characteristics of a Laser Microinterferometer", Izmeritel'naya Teknika, No. 10, pp 33-36.

7. Berthold, J. W., and Jacobs, S. F., (1970) "Ultraprecise Measurement of Thermal Coefficients of Expansion", Applied Optics, Vol. 9, No. 11 pp 2477-2480.

APPENDIX I. VALIDITY OF EQUATION (4) WHEN SOURCE IS FREQUENCY MODULATED

There may be a concern in going from Equation (3) to Equation (4). The general form of the intensity, $1 + \cos\delta$, is normally obtained from time averages of the square of the electric field. We have imposed a time variation on ν_o and thereby δ, and have used this value for finding $\cos\delta$, Eq. (5). This process would seem valid as long as $\omega_m \ll \omega_o$[1]. In this section the validity of this process is investigated.

A polarized plane wave with an electric field given by $E_o \sin\omega t$ is added to another, $E_o \sin\omega(t-t')$, where t' is the time of flight difference, 2L/c, in the arms of the interferometer. The intensity may be denoted

$$I = I_o[\sin^2\omega t\,(1+\cos\omega t')^2 + \cos^2\omega t \sin^2\omega t' - 2\sin\omega t\cos\omega t\sin\omega t'\,(1+\cos\omega t')] \quad (A1)$$

When $\omega \neq f(t)$, the time average extends over about 2×10^{-15} sec for a He-Ne laser and (A1) becomes

$$I = I_o\,(1 + \cos\omega_o t')$$

which is the standard form $\omega_o t' = \delta_o$. (If L = 10 cm, then $t' \sim 10^{-9}$ sec).

The purpose here is to time average quantities from (A1) like $\sin^2\omega t\cos^2\omega t'$ when $\omega = \omega_o + \omega_p \sin\omega_m t$. The time averages need only be extended from ν_o^{-1} to $(\nu_o + \nu_p)^{-1}$ which is trivial for laser applications since ν_p is always much less than ν_o. We now have

$$\overline{\sin^2\omega t\cos^2\omega t'} = \frac{\omega}{2\pi}\int_o^{\frac{2\pi}{\omega}} \sin^2\omega t\cos^2\omega t'\,dt$$

Integration by parts gives

$$\frac{1}{2}\cos^2\omega t' + \frac{t'}{2}\int \sin 2\omega t'\,d\omega$$

but $d\omega = \omega_p\,\omega_m \cos\omega_m t\,dt$ so that this becomes

$$\frac{1}{2}\cos^2\omega t' + \frac{\omega_p\,\omega_m t'}{2}\int_o^{\frac{2\pi}{\omega}} \sin 2\omega t'\cos\omega_m t\,dt \quad (A2)$$

If the second term is zero, one has the usual average. Now ω_m is much smaller than ω so that to first order $\cos\omega_m t$ changes very little from unity over the time of integration. Likewise $\omega t'$ is approximated by $\omega_o t' + \omega_p\omega_m t't$ and (A2) is

$$\frac{1}{2}\cos^2\omega t' + \frac{\omega_p\,\omega_m t'}{2}\left[\sin\omega_o t'\int_o^{\frac{2\pi}{\omega}} \cos\omega_p\omega_m t't\,dt + \cos\omega_o t'\int_o^{\frac{2\pi}{\omega}} \sin\omega_p\omega_m t't\,dt\right]$$

Again to first order, the second integral is zero and the first is $2\pi/\omega_o$ so that

$$\overline{\sin^2\omega t\cos^2\omega t'} = \frac{1}{2}\cos^2\omega t' + \frac{\pi\,\omega_p\,\omega_m t'}{\omega_o}\sin\delta_o$$

Other required averages to the same approximation:

$$\overline{2\cos\omega t'\sin^2\omega t} = \cos\omega t' + \frac{2\pi\omega_p\,\omega_m t'}{\omega_o}\sin\delta_o$$

$$\overline{\sin^2\omega t} = \frac{1}{2}$$

$$\overline{(1+\cos\omega t')\sin\omega t\cos\omega t\sin\omega t'} = 0$$

If one then uses δ as given in Equation (4), $\cos\delta$ is off by

$$\frac{2\pi\omega_p\,\omega_m t'}{\omega_o}\sin\delta_o$$

We have used a system with ν_p = 1 MHz, ν_m = 12.5 KHz, t' = 6 nsec, $\nu_o = 4.7 \times 10^{14}$ Hz; with $\delta_o = \pi/2$ this is $\sim 6 \times 10^{-12}$.

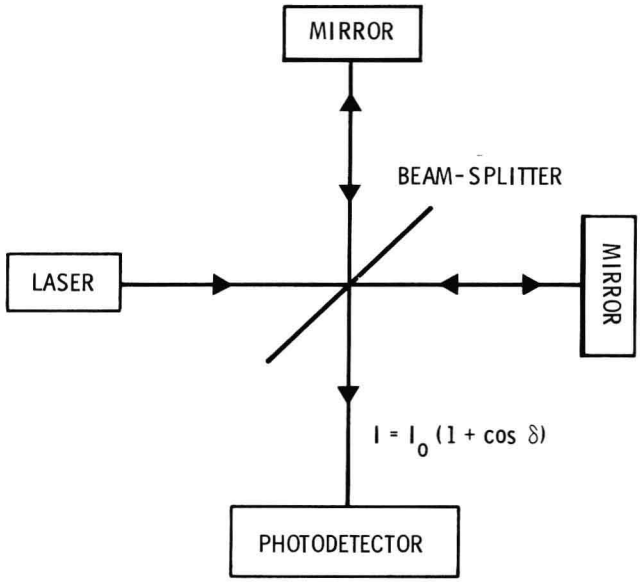

Figure 1. Basic Michelson Interferometer (not modulated)

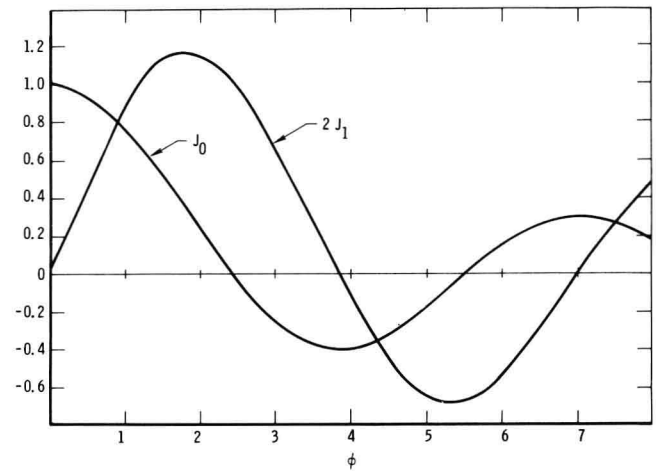

Figure 2. First and Second Bessel Functions

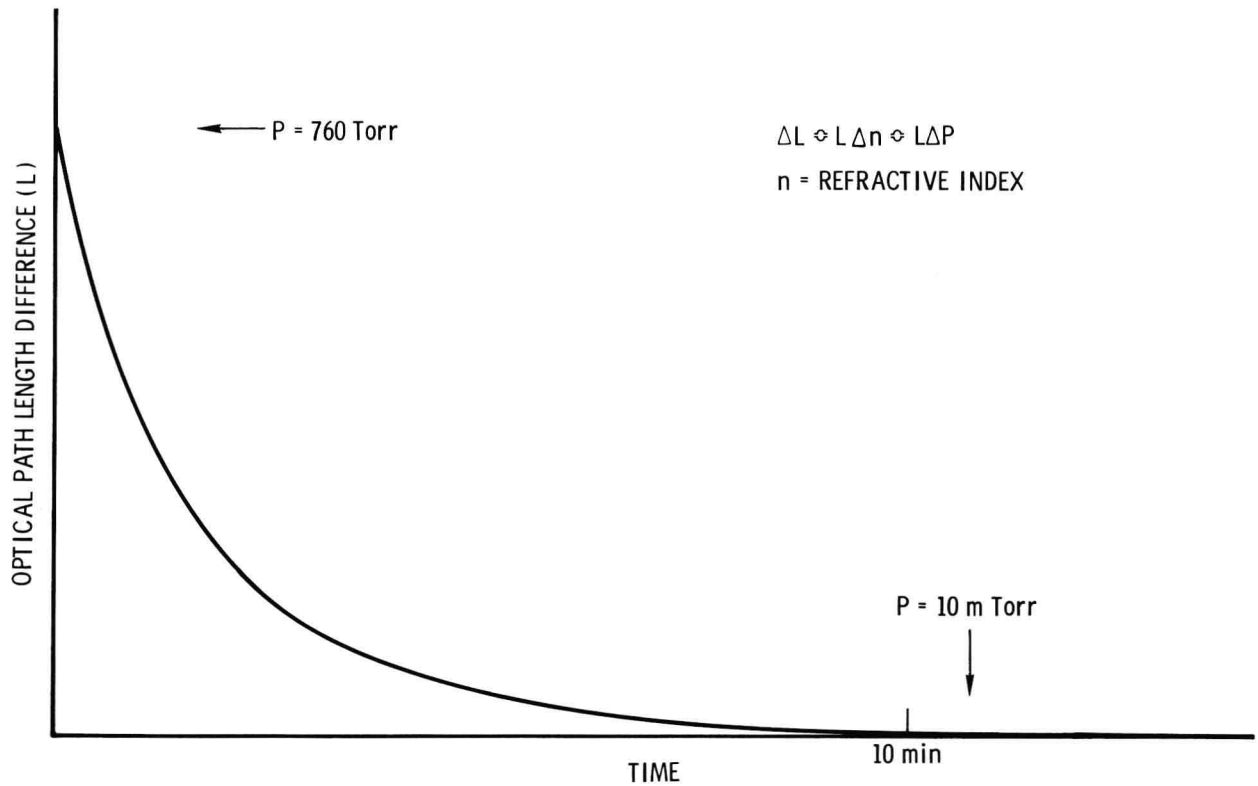

Figure 3. Change of Optical Path Length Through Decrease in Refractive Index as Air is Removed Between Interferometer Mirrors

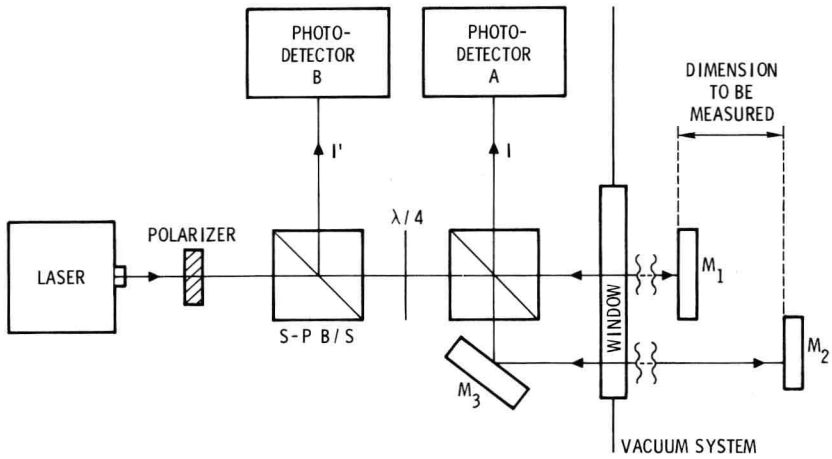

Figure 4. Laser Interferometer System Used for Measurement of Linear Displacements (between mirrors M_1 and M_2).

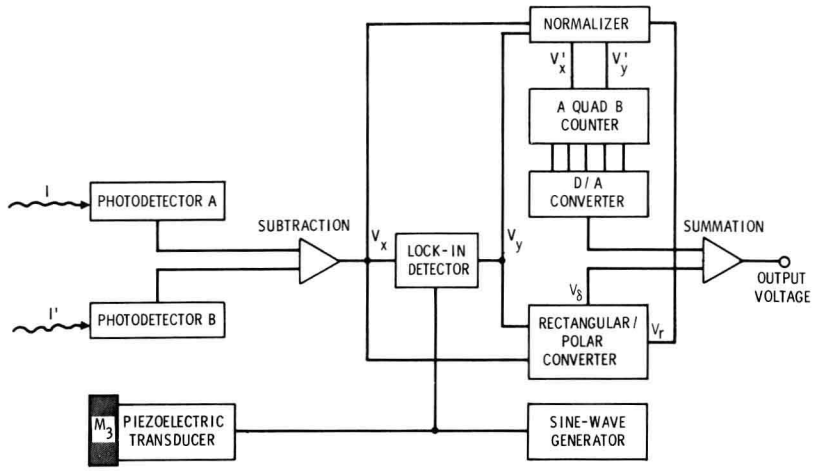

Figure 5. Electronic Signal Processing System for Use with Laser Interferometer

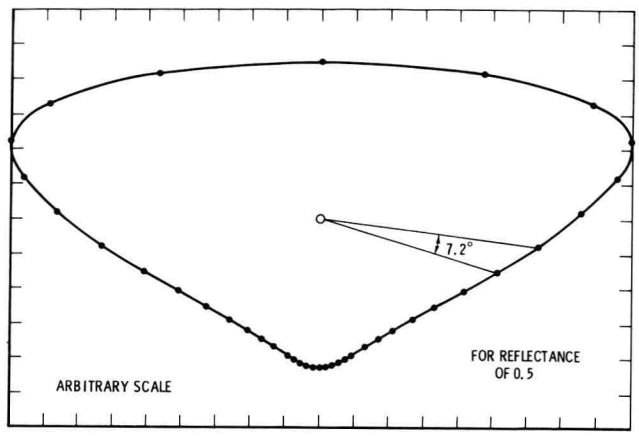

Figure 6. Equivalent Oscilloscope Display of Signals V_y and V_x for Multiple Beam (e.g. Fabry-Perot) Interferometer

SOLID PROPELLANT STRESS TRANSDUCER EVALUATION

E. C. Francis and R. E. Thompson
Chemical Systems Division

24th International Instrumentation Symposium
Instrument Society of America
Albuquerque, New Mexico

ISBN 87664-403-5

SOLID PROPELLANT STRESS TRANSDUCER EVALUATION

E. C. Francis,
Chief, Structural Research

R. E. Thompson
Research Engineer

Chemical Systems Division
United Technologies
P. O. Box 358
Sunnyvale, Calif. 94088

ABSTRACT

The accurate and reliable measurement of bond stress in a solid propellant rocket motors is a difficult task. Transducer sensing elements must be bonded to the nonlinear viscoelastic solid propellant which is a highly corrosive material and experiences large material property changes with age and temperature variation. The rocket motor bond stress changes over a broad range during storage, thermal excursions, and ignition history. An optimal stress transducer would be infinitely small, have a rigid sensing system, have high sensitivity, and exhibit excellent mechanical and electrical stability with age. This paper presents some of the engineering results obtained in the evaluation of some current state-of-the-art stress transducers.

INTRODUCTION

Bond stress measurements are required in solid propellant rocket motors to determine the reliability of U.S. missile inventories. Solid rocket motor grains tend to change properties after the motors are manufactured, causing variations in motor stress conditions which may induce structural failures. A stable and accurate bond stress transducer could be used as a gage to determine the useful service life of a rocket motor.

Modified pressure transducers have been used to measure the normal bond stresses of motors between the soft propellant and the stiff rocket motor case. Accuracy and stability of previous transducers were found to be poor since measurements could not be repeated even after short-time intervals. Two major problems occurred with early stress transducers.

1. Mechanical and electrical stability of the transducers were poor because of design and fabrication limitations and lack of chemical protection from the corrosive solid propellant material.

2. The disturbance of the propellant stress field was poorly understood and the sensing diaphragm-to-propellant interaction was not minimized to avoid nonlinear diaphragm performance.

Conversion from measured electrical signals to a meaningful stress value for the stress transducer requires structural analysis to include the effects of propellant stress disturbance, propellant interaction, and stress axiality. This type of information is provided by finite element structural analysis which includes computer modeling of the entire transducer geometry in the solid propellant medium. Results with some specific transducer designs are presented as part of this paper.

Structural analysis is conducted on all solid rocket motors to predict anticipated stress levels; however, solid rocket motor structural failures have occurred even when large margins of safety have been calculated. Development of an independent direct experimental measurement of bond stress value would bypass the limitations of the numerical stress analysis procedures and the uncertainties in the nonlinear viscoelastic properties of solid propellant and yield more accurate safety margins. These direct stress measurements can also be used to calibrate stress analysis techniques.

Laboratory Calibration Techniques and Measurement Uncertainties

Transducer calibration and data acquisition equipment, similar to that shown in Figure 1, is used to make routine electrical measurements with stress transducers. A constant current excitation source is used and monitored with a precision 10-ohm resistor inserted in the excitation line. An excitation level that produces the maximum gage output without inducing gage self-heating when in solid propellant has been determined to be 5 mA and this is maintained during calibration and transducer applications. Transducer excitation polarity must also be maintained throughout calibration and application because semiconductor strain gages exhibit some diode effects. Calibration is routinely performed with the transducer submerged in transformer oil (such as Shell Diala Oil) or similar fluid to minimize temperature fluctuation due to pressure loading. Data is recorded on a stable, accurate digital voltmeter, such as a Fluke 8800A, to insure maximum accuracy. A temperature conditioning time of three hours is used before stepwise pressure calibrations. This lengthy conditioning time is necessary to insure that the